

## Continuous digital laminography

Jeroen Cant<sup>1,2</sup>, Gert Behiels<sup>2</sup>, Jan Sijbers<sup>1</sup>

<sup>1</sup>iMinds-Vision Lab, University of Antwerp, Universiteitsplein 1, B-2610 Antwerpen, Belgium, e-mail: [jeroen.cant2@uantwerpen.be](mailto:jeroen.cant2@uantwerpen.be), [gert.behiels@agfa.com](mailto:gert.behiels@agfa.com), [jan.sijbers@uantwerpen.be](mailto:jan.sijbers@uantwerpen.be)

<sup>2</sup> Agfa Healthcare NV, Septestraat 27, B-2640 Mortsels, Belgium

### Abstract

Digital X-ray laminography is a technique for generating sectional images of an object, using an X-ray source and detector that move in opposite directions in planes above and below the object. However, motion of the X-ray source and detector during acquisition causes blurring in the projection images, which in turn leads to blurred reconstructions. To prevent these motion artifacts, both the source and detector need to be still during the X-ray pulse which leads to longer acquisition times. In this paper, we consider a system for continuous digital laminography in which the X-ray source is continuously moving and emitting, which would allow for a higher rotation speed. The inherent motion related blurring in the projections is modeled in the reconstruction algorithm. A preliminary simulation experiment comparing the classical digital laminography with the proposed continuous technique indicates that a higher reconstruction quality can be achieved near the rotation center and less streak artifacts are present, at the cost of a decreasing tangential resolution with increasing distance from the rotation center.

**Keywords:** laminography, continuous motion, algebraic reconstruction

## 1 Introduction

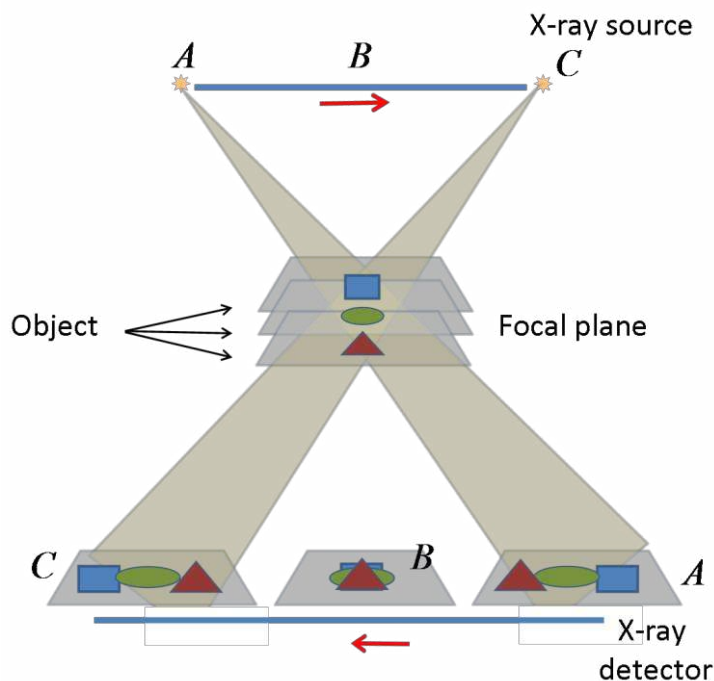


Fig. 1: Linear laminography setup

In classical laminography, a sectional image of an object is acquired by synchronously moving an X-ray tube and film during exposure on a line in opposite directions as illustrated in Fig. 1, or on a circular path with a 180° phase shift. Only the structures in the object that lie on the focal plane are projected on the same location, whereas all other structures are blurred in the projection image during the relative motion of the system. This technique was first applied in 1932 by Ziedses Des Plantes [1].

In digital laminography, a multiple of projection images are acquired in the same geometric setup with a digital detector. Sectional images at different depths can then be computed using a reconstruction algorithm. As the X-ray source only travels above the object and irradiates the object from a limited angular range, laminography reconstructions suffer from a limited depth resolution. Nevertheless, the technique is still preferred for 3D imaging in some applications, e.g. when the object to be imaged is very large and would not fit into a conventional CT scanner, or in medical imaging [2].

In this work, the effect of continuous tube and detector motion in digital laminography is studied. More specifically, continuous motion during the exposure of the individual projection images is modeled into the reconstruction algorithm. With conventional algorithms,

the blurring effects in the projection images caused by the continuous motion during the acquisition lead to blurring artifacts in the reconstruction. Recently, the algebraic iterative reconstruction technique with angular integration concept (ARTIC) was introduced [3] to reconstruct projections acquired with continuous tube motion and emission. In this work, the use of ARTIC in digital laminography is explored. We first provide an outline of the algorithmic ideas behind ARTIC. Next, the extension of ARTIC towards laminography is described, which will be referred to as continuous laminography. Finally, by means of simulation experiments on the XCAT phantom [4] we demonstrate the value of the proposed method.

## 2 Method

In its algebraic form, a step-and-shoot reconstruction problem can be written as a linear set of equations

$$Wv = p,$$

in which  $v \in \mathbb{R}^n$  is the unknown rasterized representation of the reconstructed object;  $p \in \mathbb{R}^{ld}$  contains the measured projection data with  $l$  the number of projection angles and  $d$  the number of detectors in each projection; and  $W \in \mathbb{R}^{ld \times n}$  represents the projection matrix of the scanning geometry. Define  $W_i \in \mathbb{R}^{d \times n}$  as the rows of the projection matrix corresponding to the  $i$ 'th exposure. Also define the function  $\omega_\theta : \mathbb{R}^n \rightarrow \mathbb{R}^d$  as the projection of an object under the angle  $\theta$ . With a step-and-shoot acquisition mode, each exposure image  $W_i v$  contains the projection of the object in the direction  $\theta_i$ :  $W_i v = \omega_{\theta_i}(v)$ , for which conventional reconstruction techniques apply.

For continuous acquisition, however, each exposure image is formed by continuously irradiating the object from all angles in the range  $[\theta_i, \theta_{i+1}]$ . The continuous projection operation can be approximated [3] by sampling the angular range in  $S$  intervals:

$$W_i v = \frac{1}{S} \sum_{\alpha=0}^{S-1} \omega_{\alpha_i}(v).$$

This way, a new projection matrix can be constructed ready for use in any algebraic reconstruction technique.

## 3 Experiments

To validate the use of ARTIC for digital laminography, a simulation experiment was performed using the XCAT [4] phantom in a linear laminography setup. Step-and-shoot and continuous projections were simulated, both covering 10 projections in an angular range of  $40^\circ$ . Detector and X-ray source moved in parallel planes on opposite sides of the phantom, as illustrated in Fig.2. The source image distance was set to 1200mm and the rotation center of the source and detector motion was placed in the middle of the phantom. Poisson noise was simulated in both sets of projections, assuming an incident photon count of  $I_0=100000$ . The step-and-shoot and continuous projections were reconstructed with SIRT and ARTIC respectively, using the open source ASTRA toolbox [5,6].

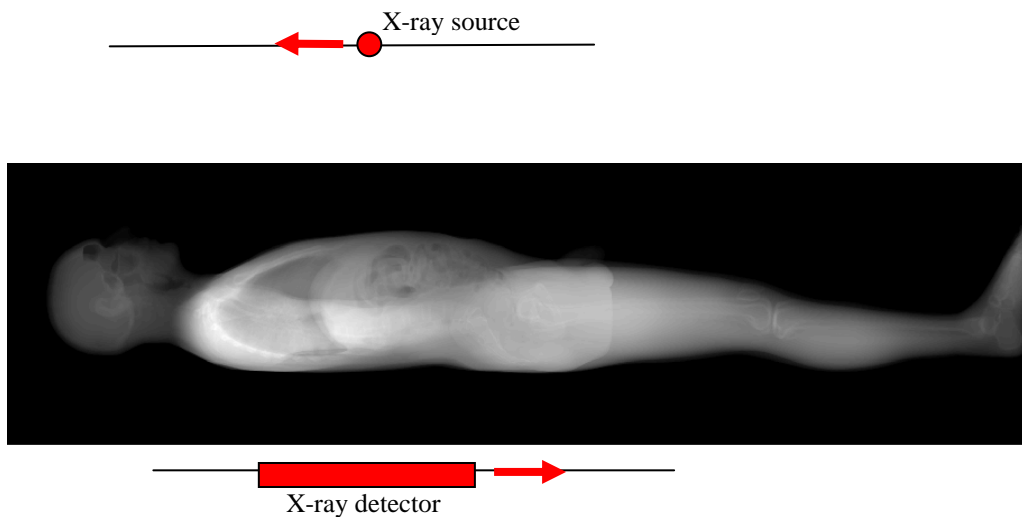


Fig. 2: Geometry for the experiment with the XCAT phantom. A flat panel detector moves continuously in a plane underneath the phantom, while the X-ray source moves in opposite direction in a plane above the phantom.

Conventional reconstructions from a limited angle suffer from limited depth resolution, even when a high amount of noiseless projections are provided. Especially structures with edges which are, due to the limited angle, not oriented parallel to the direction of incoming rays [7] in any projection, are almost invisible in the reconstructed image. The red arrow in Fig. 3a illustrates such a structure. The goal of this experiment however, is not to improve depth resolution. In this work, the primary goal is to reduce the number of projections and thus increase the acquisition speed by continuous motion and emission of the X-ray tube and detector. Therefore, a SIRT reconstruction from 300 noiseless projections from the same angular range of  $40^\circ$  was computed and is further considered as the reference. This reference reconstruction still contains reconstruction artifacts, due to the limited angle acquisition, as can be observed in Fig 3b.

A reduction of the number of projections and the addition of noise will further reduce the reconstruction quality. In the following experiment, conventional SIRT and ARTIC reconstructions using only 10 noisy step-and-shoot resp. continuous projections are compared to this reference reconstruction.

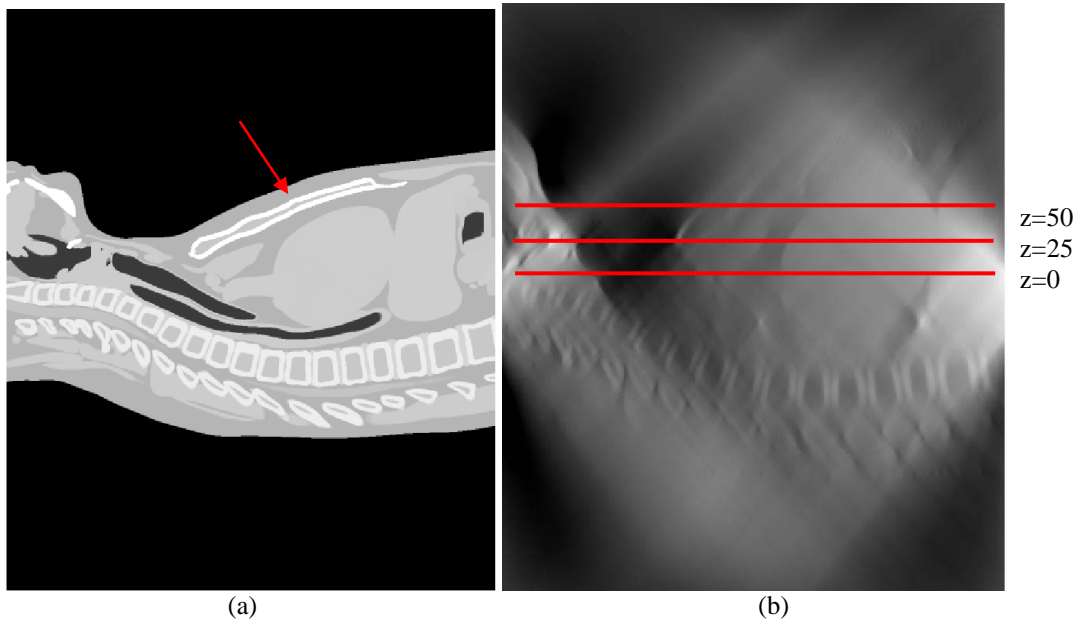


Fig. 3. (a) sagittal (side) view through the middle of the XCAT phantom. The arrow indicates a structure with edges perpendicular to the incoming rays. (b) sagittal view through the reference SIRT reconstruction with 300 noiseless projections, showing limited depth resolution. The red lines indicate the location of the 3 reference slices at different depths. The slice at  $z=0$  represents the slice in the rotation center of the continuous tube-detector motion.

Both SIRT and ARTIC reconstructions were stopped at the iteration during which the middle slice reached the lowest root mean squared error (RMSE) compared to the reference reconstruction with 300 noiseless projections. The RMSE per slice of both SIRT and ARTIC reconstructions is displayed in Fig.4. The largest improvement in RMSE is observed near the rotation center.

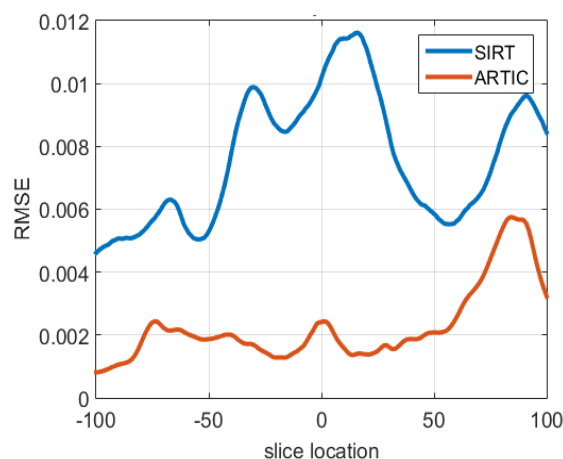


Fig. 4: RMSE per slice

The reference reconstruction and the resulting SIRT and ARTIC reconstructions are displayed in Fig. 5. Note how, despite the limited depth resolution, the reference reconstruction is still capable of providing high resolution section images (Fig. 5 a,d,g). The reduction of the number of projections causes blurring and ringing artifacts in the SIRT reconstruction, which are caused by streak artifacts in the Z dimension. Furthermore, truncation artifacts can be observed near the top and bottom of the SIRT reconstruction at a depth of  $z=50$ . The ARTIC reconstruction near the rotation center are displayed in Figs. 5c,f,i.

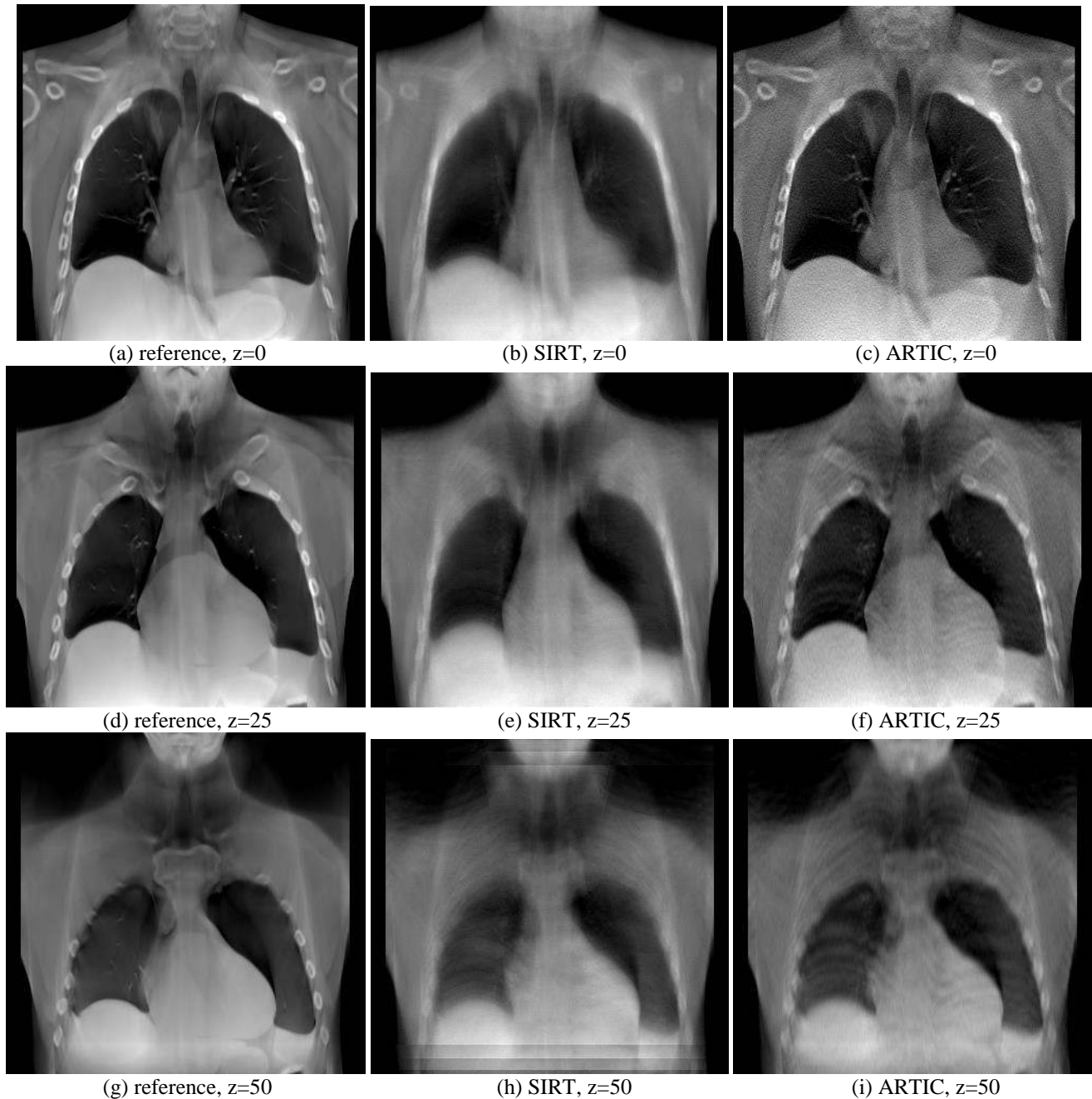


Fig. 5: Reconstructions of the XCAT phantom, all taken with angular range of  $40^\circ$ . First column: SIRT reconstruction from 300 noiseless projections (considered the reference image). Middle column: SIRT reconstructions from 10 noisy step-and-shoot projections. Right column: ARTIC reconstructions from 10 noisy continuous projections.

## 4 Discussion

The experiment illustrates that the SIRT reconstruction quality in the slices near the rotation center (Fig. 5b) is substantially improved by ARTIC (Fig. 5c), whereas in slices further away from the rotation center ARTIC shows increased blurring in the direction of the tube motion (Fig. 5i) compared to SIRT (Fig. 5h). The RMSE shows a large improvement on slices near the rotation center, but also moderate improvements away from the center with ARTIC. As the phantom content varies strongly between slices, the slice location dependent resolution of this technique should be more thoroughly evaluated with a resolution phantom or MTF measurements in future work.

The effect of ARTIC on the reconstruction quality can be understood intuitively from the central slice theorem. For parallel beams, the Fourier transform of a projection along angle  $\theta_n$  corresponds to a line in the Fourier transform of the image, as illustrated in Fig. 6. If the angular distance  $\Delta$  between subsequent projections is increased, this results in a coarser sampling of the Fourier domain and thus more reconstruction artifacts. If however projections are acquired continuously, information from the entire wedge of width  $\Delta$  in the Fourier domain is collected. The ARTIC reconstruction algorithm subsequently fills up this entire wedge in the reconstruction process, leading to a decreased number of artifacts, especially near the rotation center. For cone beam CT, a similar reasoning leads to an increased number of artifacts due to a coarser sampling of the 3D Fourier domain of the object.

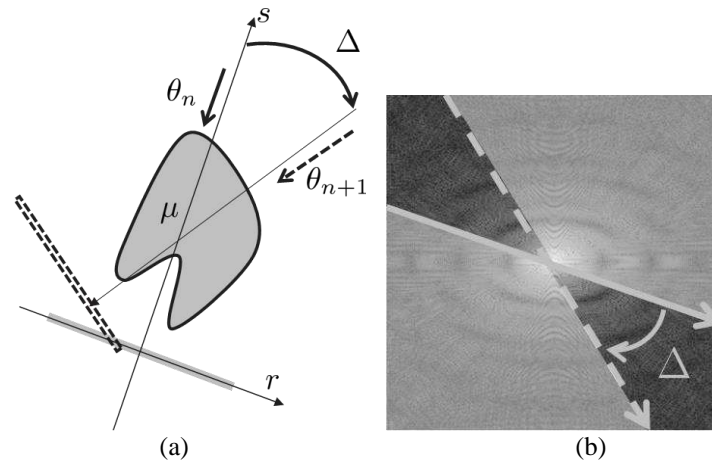


Fig. 6 (a) Illustration of parallel beam acquisition. (b) The imaged object in the Fourier domain.

Continuous laminography can be of particular interest in systems where the read out speed of the flat panel detector is the limiting factor on the acquisition speed. In this case, the total acquisition time can only be reduced by reducing the number of projections. If a high resolution is primarily needed in a specific region of interest of the image, ARTIC provides a trade off between acquisition speed and region of interest size.

## 5 Conclusion

We have shown that performing digital laminography while keeping the x-ray source and detector in a continuous motion and continuous exposure strongly increases the reconstruction quality near the rotation center, at the cost of moderate blurring effects further away from the center. The method described in this work is of interest in laminography studies where a faster acquisition is demanded, especially if reconstruction quality is required in a specific region of interest.

## References

- [1] Z. des Plantes, Eine neue Methode zur Differenzierung in der Röntgenographie, Acta Radio., 13, p.182, 1932
- [2] Dobbins, J. T., & Godfrey, D. J., Digital X-ray tomosynthesis: current state of the art and clinical potential. *Physics in Medicine and Biology*, 48(19), R65–R106, 2003
- [3] J. Cant et al, Modeling blurring effects due to continuous gantry rotation: Application to region of interest tomography, *Med. Phys.*, 42(5), pp. 2709–2717, 2015
- [4] W.P. Segars et al, Realistic CT simulation using the 4D XCAT phantom. *Med. Phys.*, 35(8), pp. 3800–3808, 2008.
- [5] W. van Aarle, et al, "The ASTRA Toolbox: a platform for advanced algorithm development in electron tomography", *Ultramicroscopy*, 157, pp. 35-47, 2015.
- [6] W J. Palenstijn, K. J. Batenburg, and J. Sijbers, "The ASTRA Tomography Toolbox", 13th International Conference on Computational and Mathematical Methods in Science and Engineering, CMMSE 2013, vol. 4, pp. 1139-1145, 2013
- [7] Clackdoyle, R., & Defrise, M, Tomographic Reconstruction in the 21st Century. *IEEE Signal Processing Magazine*, 27(4), 60–80, 2010